Available online at www.sciencedirect.com
ScienceDirect
Procedia Manufacturing 47 (2020) 440–444
Procedia MANUFACTURING
www.elsevier.com/locate/procedia

23rd International Conference on Material Forming (ESAFORM 2020)

Integrated Manufacturing of AA6082 by Friction Stir Welding and Incremental Forming: Strain Analysis of Deformed Samples

Felice Rubino[a], Vitantonio Esperto[a], Rui Miguel Ferreira Paulo [b], Fausto Tucci[c], Pierpaolo Carlone[c]*

[a]*Department of Chemical, Materials and Production Engineering, University of Naples Federico II, Piazzale Tecchio, 80, Napoli (NA), Italy.*
[b]*School of Mechanical and Aerospace, Queen's University Belfast, United Kingdom.*
[c]*Department of Industrial Engineering, University of Salerno, Via Giovanni Paolo II, 132-84084 Fisciano (SA), Italy.*

* Corresponding author. Tel.: +39-089964310 *E-mail address:* pcarlone@unisa.it

Abstract

Flexible manufacturing systems have attracted increasing interest especially to produce highly customized components or for manufacturing of prototypes/small batches. Among others, the single point incremental forming (SPIF) process has been successfully applied in several non-structural applications, e.g. architectural lining, decorative element manufacturing and rapid prototyping. Nevertheless, accuracy, toolpath definition and reduced productivity are still relevant issues, in particular when tailored banks are processed. The present work discusses an integrated manufacturing route combining welding and forming of aluminum sheets. More specifically, attention has been focused on the strain distribution induced by the single point incremental forming of friction stir welded AA6082 sheets. The used method consists in the generation of digital 3D twins of the undeformed and deformed shapes by means of ScanProbe and Matlab software packages. The displacement field, evaluated from the comparison between initial and final positions of surface points, is then used as input in a FE model that estimates the final strain distribution. Forming limit diagrams (FLD) have been evaluated for welded sheets and compared to the forming limit curve of conventional forming processes. Obtained results have been finally compared with strain distributions detected in fusion welded sheets.

Keywords: Taylored blanks; Friction stir welding; Single point incremental forming; Forming limit diagram.

1. Introduction

Rapid advances in industrial design and engineering imply an ever-growing requirement for new materials and components, capable to fulfill singular challenging needs. In the last few decades, manufacturing engineering has responded to these challenges using a variety of different approaches, such as, for instance, developing new metallic alloys [1], advanced composite materials [2], or new surface treatment techniques [3,4]. One of the most flexible solution to satisfy many industrial requirements are the tailored blanks [5]. This definition is used to describe components made from one or more sheets joined together by advanced welding techniques, presenting variable materials, thickness, strength or coating and complex shapes [5,6]. The welding techniques adopted are one of the key points in manufacturing of tailored blanks. In this framework, the friction stir welding (FSW) is attracting particular interest. FSW is a solid-state welding technique to produce high-quality joints [7–9]. FSW is employed to weld a wider range of metallic alloys, if compared to conventional fusion welding processes [7]. Moreover, by means of the FSW

10.1016/j.promfg.2020.04.331

technology, it is possible to produce dissimilar welds with reduced defects [10–12].

The complex shapes are another pillar of the tailored blanks definition. These shapes can be achieved by conventional forming processes using expensive tools. Nevertheless, this approach is extremely inconvenient for small batch production of this kind of components. Single point incremental forming (SPIF) can be employed to shape thin blanks avoiding expensive tools [13,14]. SPIF is an extremely flexible technique, based on the usage of a forming punch, moved by a numerically controlled machine, to locally deform a metallic sheet. The sheet is typically clamped using an appropriate blank holder [15]. The forming performance of this technique, in terms of deformations, result remarkably higher if compared to the conventional stamping processes [13,16,17]. The application of SPIF on FSW welded blanks is attracting growing interest within the scientific and industrial communities, meaning that several studies and projects have been focused on it [18,19].

In the present work, AA6082 thin blanks have been welded by FSW technique, using different working parameters, and then formed until the material failure, by single point incremental forming. The local strain have been numerically evaluated using ABAQUS commercial suite. The deformations have been analyzed to achieve the forming limit diagrams, relatively to each of the produced joints.

2. Materials and methods

The welding processes described in the present work have been performed considering, as a first attempt, similar AA6082 blanks. The welded sheets are 220 mm in length, 110 mm in width and 2 mm in thickness. The blanks were butt-welded along the longer dimension. Several joints were produced by FSW and by tungsten inert gas (TIG) welding. The friction stir welds were performed using an HSS cylindrical tool with a shoulder diameter of 20 mm and a conical pin characterized by an angle of 15° and a height of 1.8 mm. The experiment plan has been designed defining three levels for both the advancing velocity and the spindle speed. Table 1 summarizes a scheme of the friction stir welded joints, reporting the employed parameters. Fig. 1 presents a representative friction stir welded joint.

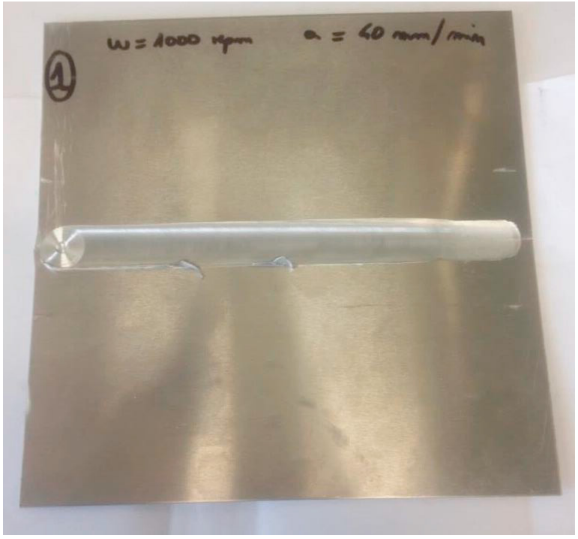

Fig. 1. Representative friction stir welded butt weld.

The surfaces of the blanks were marked before the forming process, in order to evaluate the local deformation after SPIF. All the blanks have been formed imposing the same tool path: a converging circular spiral (Fig. 2). In each of the forming processes, the tool was stopped at the material failure. A representative picture of a formed blank (at rupture) is shown in fig. 3. In order to assess the formability of the friction stir welded joints, the same procedure has been performed on TIG welded blanks with the same dimensions.

Table 1. Friction stir welding parameters.

Samples	Advancing velocity [mm/min]	Spindle speed [rpm]
1	40	1000
2	100	1000
3	70	1200
4	40	1400
5	100	1400

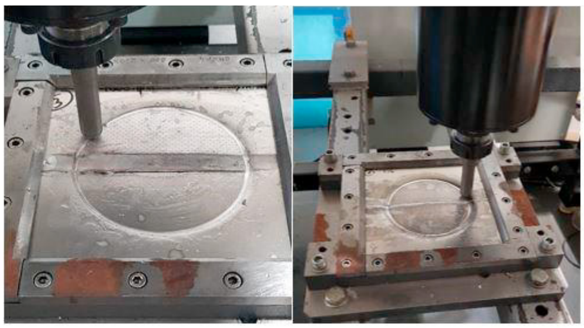

Fig. 2. Single point incremental forming of friction stir welded blanks.

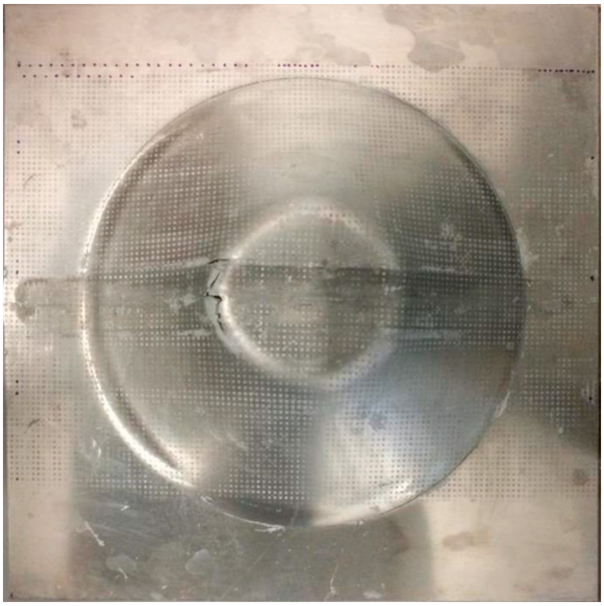

Fig. 3. Representative picture of a single point incremental formed blank.

A three-dimensional digital twin of each deformed surface has been created using a photographic acquisitions system controlled by the software ScanProbe (Fig. 4).

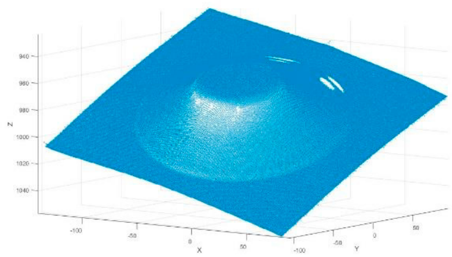

Fig. 4. Digital twin of a deformed blank.

The acquired point clouds have been rotated and translated, in Matlab environment, to measure the displacement of the markers with respect to their initial position. In order to evaluate the strain field, the measured displacements were implemented in a numerical model, developed using Abaqus suite (Fig. 5). The blank has been discretized using four node reduced shell elements (S4R), characterized by five integration points along the thickness of 2 mm. In order to compute precisely the deformations at the marker position, each node of the mesh corresponds to a marker. Each single point displacement has been implemented as a boundary condition for each node of the mesh. All the displacements are imposed at the same time in a unique step, following a linear path from the initial to the deformed configuration. All the degrees of freedom were constrained at the edges of the blank, to reproduce the clamp fixture.

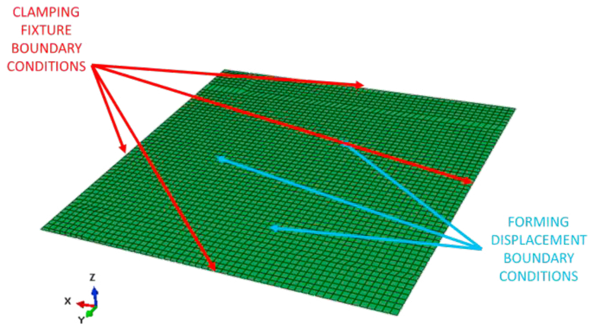

Fig. 5. Domain discretization and implemented boundary condition.

3. Results and discussion

The maximum depth achieved in SPIF, for different conditions of the blank, are reported in Table 2. A higher value for the maximum depth indicates higher formability of the friction stir welded blank. The final forming depth coincides with the material failure, and, therefore, with the material formability limit. The TIG welding exhibits a remarkably lower formability. The data reported in Table 2 evidence a pronounced sensitivity to the advancing velocity, when compared with the spindle speed. It is worth to note that the failure occurred more frequently on the welding line (Fig. 6) than on the base material (Fig. 7). In these cases, the friction stir welded line results more formable than the base material.

Table 2. Maximum forming depth and failure location after SPIF with different blanks.

Samples	Advancing velocity [mm/min]	Spindle speed [rpm]	Maximum forming depth [mm]	Failure location
1	40	1000	36.50	Welding line
2	100	1000	18.06	Welding line
3	70	1200	40.76	Base material
4	40	1400	39.67	Base material
5	100	1400	21.63	Welding line
TIG	/	/	15.20	Welding line

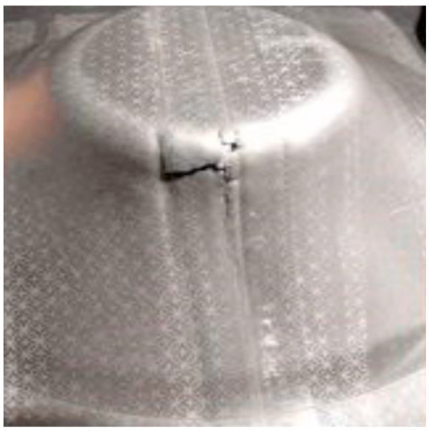

Fig. 6. Welding line failure.

Fig. 7. Base material failure.

Figures 8 and 9 report the numerical results of the distribution of major and the minor strains, evaluated on a representative FSW blank, for which failure occurred on the base material. The major strain direction corresponds to the radial one, with respect to the tool spiral trajectory. It attains a remarkably high value at the maximum depth. The minor strain direction corresponds to the tangential one, with respect the spiral trajectory. In both figures, a strain peak can be observed at the crack position. Excluding the crack neighborhood, the tangential strain shows a homogeneous distribution in the deformed region.

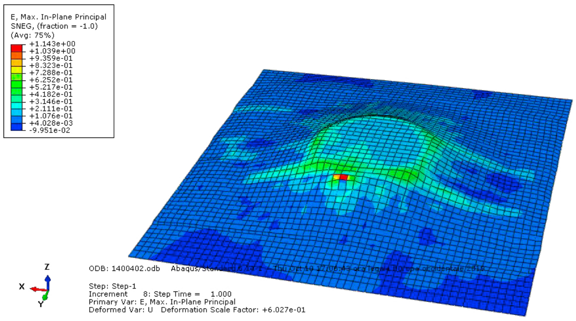

Fig. 8. Contour plot of the major strain distribution.

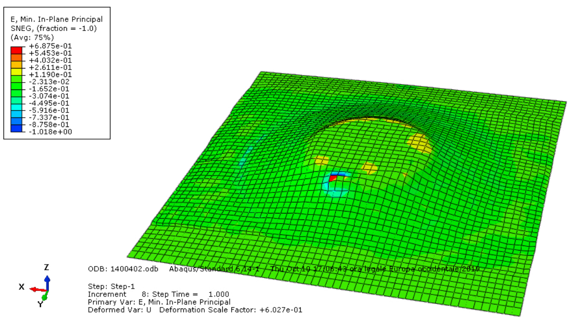

Fig. 9. Contour plot of the minor strain distribution.

Fig. 10 summarizes the forming limit diagrams of all investigated samples. The plotted data are a selection of strain values randomly collected in the most deformed zone of each dataset. The strain values in the neighborhood of the failure have been excluded in this diagram. The data are compared to the forming limit curve relative to conventional forming processes [13,14]. In almost all cases, the material reaches formability levels higher than the conventional FLC. The reported results are compliant with the maximum depth observed and reported in Table 2: the samples achieving higher maximum depth present higher strain values. The FSW blanks formability results are highly influenced by the advancing velocity. Indeed, the welds produced at 100 mm/min exhibit, in general, lower formability. Comparing the samples welded using the same advancing velocity, a better formability has been achieved using higher spindle speed. During the FSW process, higher advancing velocity implies lower mixing time of the crystal lattice and faster temperature decrease after the passage of the welding tool. Higher spindle speed increases the temperature and enhances the material softening during welding [20]. TIG welded strains are remarkably lower than the ones observed on good quality FSW welds.

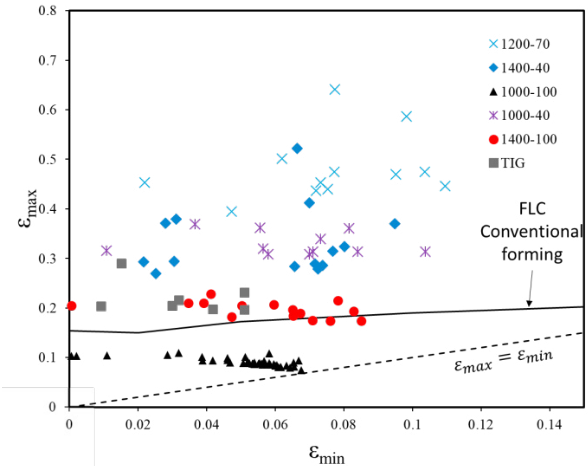

Fig. 10. Formability limit diagram of the welded blanks.

4. Conclusions

In conclusion, the present manuscript presents the assessment of formability of SPIF AA6082 blanks, with 2 mm thickness, butt-welded by FSW process. The analysis of the strain distributions, conducted using digital twins of the formed blanks, evidenced the following hypotheses:

- In good quality welds, the material failure during SPIF occurs in the base material, evidencing that the mechanical properties of the welds are equal or better than the ones of the original material;
- In the analyzed friction stir welded joints, the advancing speed is the main factor in the quality of the joint;
- Higher advancing velocity values negatively affects the blank formability, while higher spindle speed promotes the weld formability;
- TIG welded joints exhibited remarkably lower properties, compared to the FSW welds.

References

[1] Kipouros GJ, Caley WF, Bishop DP. On the advantages of using powder metallurgy in new light metal alloy design. Metall Mater Trans A Phys Metall Mater Sci 2006;37:3429–36.

[2] Carlone P, Rubino F, Paradiso V, Tucci F. Multi-scale modeling and online monitoring of resin flow through dual-scale textiles in liquid composite molding processes. Int J Adv Manuf Technol 2018.

[3] Tucci F, Esperto V, Rubino F. Surface Induction Hardening of Steels : Process Modelling and Numerical Simulation. Key Engineering Materials, 2019;813:399-403

[4] Paradiso V, Rubino F, Tucci F, Astarita A, Carlone P. Thermo-mechanical modeling of laser treatment on titanium cold-spray coatings. AIP Conf. Proc., vol. 1960, 2018.

[5] Merklein M, Johannes M, Lechner M, Kuppert A. A review on tailored blanks - Production, applications and evaluation. J Mater Process Technol 2014;214:151–64.

[6] Padmanabhan R, Oliveira MC, Menezes LF. Deep drawing of aluminium-steel tailor-welded blanks. Mater Des 2008;29:154–60.

[7] Carlone P, Astarita A, Rubino F, Pasquino N. Microstructural Aspects in FSW and TIG Welding of Cast ZE41A Magnesium Alloy. Metall Mater Trans B Process Metall Mater Process Sci 2016;47:1340–6.

[8] Rubino F, Scherillo F, Franchitti S, Squillace A, Astarita A, Carlone P. Microstructure and surface analysis of friction stir processed Ti-6Al-4V plates manufactured by electron beam melting. J Manuf Process 2019;37:392–401.

[9] Mehta KP, Carlone P, Astarita A, Scherillo F, Rubino F, Vora P. Conventional and cooling assisted friction stir welding of AA6061 and AZ31B alloys. Mater Sci Eng A 2019;759:252–61.

[10] Mehta KP, Badheka VJ, Mehta KP, Badheka VJ. A Review on Dissimilar Friction Stir Welding of Copper to Aluminum : Process , Properties , and Variants A Review on Dissimilar Friction Stir Welding of Copper to Aluminum : Process , Properties , and Variants. LMMP 2016;31:233–54.

[11] Boccarusso L, Astarita A, Carlone P, Scherillo F, Rubino F, Squillace A. Dissimilar friction stir lap welding of AA 6082 - Mg AZ31: Force analysis and microstructure evolution. J Manuf Process 2019;44:376–88.

[12] Paradiso V, Rubino F, Carlone P, Palazzo GS. Magnesium and Aluminium alloys Dissimilar Joining by Friction Stir Welding. Procedia Eng 2017;183:239–44.

[13] Duflou JR, Habraken A, Cao J, Malhotra R, Bambach M, Adams D, et al. Single point incremental forming : state-of-the-art and prospects 2018:743–73.

[14] Jeswiet J, Micari F, Hirt G, Bramley A, Duflou J, Allwood J. Asymmetric Single Point Incremental Forming of Sheet Metal n.d.;1.

[15] Silva MB, Nielsen PS, Bay N, Martins PAF. Failure mechanisms in single-point incremental forming of metals. Int J Adv Manuf Technol 2011;56:893–903.

[16] Madeira T, Silva CMA, Silva MB, Martins PAF. Failure in single point incremental forming. Int J Adv Manuf Technol 2015;80:1471–9.

[17] Emmens WC, Boogaard AH Van Den. An overview of stabilizing deformation mechanisms in incremental sheet forming 2009;209:3688–95.

[18] Silva MB, Skjoedt M, Vilaça P, Bay N, Martins PAF. Single point incremental forming of tailored blanks produced by friction stir welding. J Mater Process Technol 2009;209:811–20.

[19] Tucci F, Angelo R, Valente F, Sousa RJA De, Rubino F, Carlone P. A Finite Element Approach to the Integrated Modelling of the Incremental Forming of Friction Stir Welded Sheets. AIP Conference Proceedings 2019;2113:06005.

[20] Paulo RMF, Carlone P, Paradiso V, Valente RAF, Teixeira-Dias F. Prediction of friction stir welding effects on AA2024-T3 plates and stiffened panels using a shell-based finite element model. Thin-Walled Struct 2017;120:297–306.